OXFORD

Integrative Biology, 2021, 13(2),31–43

doi: 10.1093/intbio/zyaa027
Advance Access publication January 30, 2021
Original Article

ORIGINAL ARTICLE

Pericyte migration and proliferation are tightly synchronized to endothelial cell sprouting dynamics

Laura Beth Payne[1,†], Jordan Darden[1,2,†‡], Ariana D. Suarez-Martinez[3,†], Huaning Zhao[1,4,‡], Alissa Hendricks[2], Caitlin Hartland[1,‡], Diana Chong[5], Erich J. Kushner[6], Walter L. Murfee[3], and John C. Chappell[1,2,4,7,*]

[1]Center for Heart and Reparative Medicine Research, Fralin Biomedical Research Institute, Roanoke, VA 24014, USA, [2]Graduate Program in Translational Biology, Medicine, & Health, Virginia Polytechnic Institute and State University, Blacksburg, VA 24061, USA, [3]J. Crayton Pruitt Family Department of Biomedical Engineering, University of Florida, Gainesville, FL 32611, USA, [4]Department of Biomedical Engineering and Mechanics, Virginia Polytechnic Institute and State University, Blacksburg, VA 24061, USA, [5]Department of Biology, The University of North Carolina at Chapel Hill, Chapel Hill, NC 27599, USA, [6]Department of Biological Sciences, University of Denver, Denver, CO 80208 USA, and [7]Department of Basic Science Education, Virginia Tech Carilion School of Medicine, Roanoke, VA 24016, USA

***Corresponding author**. E-mail: JChappell@vtc.vt.edu
[†]Authors contributed equally to this work.
[‡]Previous affiliations.

Abstract

Pericytes are critical for microvascular stability and maintenance, among other important physiological functions, yet their involvement in vessel formation processes remains poorly understood. To gain insight into pericyte behaviors during vascular remodeling, we developed two complementary tissue explant models utilizing 'double reporter' animals with fluorescently-labeled pericytes and endothelial cells (via *Ng2:DsRed* and *Flk-1:eGFP* genes, respectively). Time-lapse confocal imaging of active vessel remodeling within adult connective tissues and embryonic skin revealed a subset of pericytes detaching and migrating away from the vessel wall. Vessel-associated pericytes displayed rapid filopodial sampling near sprouting endothelial cells that emerged from parent vessels to form nascent branches. Pericytes near angiogenic sprouts were also more migratory, initiating persistent and directional movement along newly forming vessels. Pericyte cell divisions coincided more frequently with elongating endothelial sprouts, rather than sprout initiation sites, an observation confirmed with *in vivo* data from the developing mouse brain. Taken together, these data suggest that (i) pericyte detachment from the vessel wall may represent an important physiological process to enhance endothelial cell plasticity during vascular remodeling, and (ii) pericyte migration and proliferation are highly synchronized with endothelial cell behaviors during the coordinated expansion of a vascular network.

Key words: pericyte; endothelial cell; angiogenesis; cell migration; proliferation; time-lapse imaging

Received June 24, 2020; **revised** November 13, 2020; **editorial decision** December 26, 2020; **accepted** December 26, 2020

INSIGHT BOX

In the current work, we harnessed the power of time-lapse imaging to capture the dynamic crosstalk between endothelial cells and pericytes during key phases of blood-vessel formation. Complementary adult and embryonic tissue explant models harboring reporters for each cell type revealed distinct yet integrated cellular behaviors during vascular remodeling. Within angiogenic vascular networks, a subset of pericytes detached from the vessel wall and migrated into the interstitial space in a phase of 'pericyte shedding' that may be functionally relevant during vessel remodeling in physiological and pathological settings. Pericyte migration and proliferation were also tightly coordinated with the behaviors of adjacent endothelial cells, highlighting the need to consider the contributions of both cell types in angiogenesis models.

INTRODUCTION

Angiogenic sprouting yields new blood vessels from pre-existing microvasculature. This multistage process involves collective endothelial cell migration [1, 2] orchestrated by dynamic cellular and molecular interactions across organ systems throughout development [3]. Endothelial cells receive and integrate proangiogenic cues from their local environment, coordinating the outward migration of an endothelial 'tip' cell with the expansion of adjacent 'stalk' cells that maintain the growth of the nascent vessel branch [4–7]. Although the tightly regulated, homotypic interactions among endothelial cells are known to be critical for successful angiogenic remodeling [8], the heterotypic interactions between endothelial cells and microvascular pericytes during angiogenesis are still being resolved at a more fundamental level. Pericytes stabilize quiescent microvasculature [9–11], among other critical functions [12], but during angiogenesis these specialized vascular cells can extend their coverage to the base of filopodia extending from endothelial tip cells [13, 14]. This close apposition to sprouting endothelial cells suggests that pericytes may be more prominently and uniquely involved in the different stages of angiogenic remodeling than previously appreciated.

For existing microvessels to begin remodeling, especially in adult tissues, the vessel wall must undergo a phase of coordinated disassembly [15–17], conveying a level of plasticity to endothelial cells in their response to angiogenic cues. Pericyte disengagement from the capillary wall is therefore likely to be an important and necessary component of this initial vessel deconstruction, as it facilitates the emergence of a sprouting endothelial cell [18]. However, similar to many angiogenic mechanisms [19], this process must be kept within a narrow physiological range. Misregulated and excessive pericyte divestment may ultimately become a contributing factor to disease pathogenesis. In proliferative diabetic retinopathy, for example, pericyte 'dropout' is a key clinical feature for disease progression [20]. Pericyte detachment has also been observed in fibrotic pathologies, most notably in the lungs and kidneys where detached pericytes are believed to exacerbate tissue fibrosis along with, or perhaps acting as, interstitial fibroblasts [21, 22]. Thus, although pericytes migrate away from the vessel wall in certain clinical disorders, this behavior might also constitute an important early phase of angiogenic remodeling, allowing adjacent endothelial cells to initiate sprouting from a parent vessel.

Preceding their divestment from the capillary wall, pericytes must dissolve the specialized extracellular matrix (ECM) surrounding themselves and the endothelium, often referred to as the vascular basement membrane (vBM). Pericytes are known to secrete matrix metalloproteinases (MMPs) such as MMP2, MMP3 and MMP9 during physiological angiogenesis as well as in certain pathological scenarios [16, 23–26]. Being embedded in the vBM of a quiescent microvascular network does not permit a high level of pericyte migration under homeostatic conditions. Pericytes are therefore assumed to be largely stationary and nonmigratory unless stimulated. Consistent with this idea is the observation that cellular extensions from adjacent pericytes, and not the pericyte somas themselves, reinvest and cover a region of the microvessel wall following pericyte ablation by high-power laser radiation [27]. Thus, it appears that pericyte migration along the capillary wall occurs primarily in the context of active angiogenesis and vessel remodeling [28–32], and less so along quiescent vascular networks that lose pericyte coverage in the absence of angiogenic stimulation. Additional studies will be necessary, though, to better understand pericyte migration dynamics across a range of physiological and pathological scenarios.

In addition to migrating along the microvasculature, pericytes can also divide and proliferate to expand their coverage of blood vessels where necessary. Certain chronic illnesses such as proliferative diabetic retinopathy and Alzheimer's Disease have been suggested to involve a large component of pericyte loss from the vessel wall [20, 33–35]. In these settings, it might be advantageous to therapeutically target pericyte proliferation and migration as a means to restore their coverage and stabilization of vulnerable capillary networks. Targeted delivery of growth factors such as platelet-derived growth factor-BB (PDGF-BB), fibroblast growth factor-2, and/or heparin-binding epidermal growth factor-like growth factor (HB-EGF) may be able to drive pericyte proliferation [36]. However, pericytes may require multiple cues to initiate cell division (e.g. expanding angiogenic networks), as pericyte ablation experiments in the mouse brain suggest that pericytes do not divide to replace lost pericytes but simply extend cellular processes to re-establish vessel coverage [27]. Therefore, it is critical to continue developing cutting-edge models [28, 30, 37] and tools [27, 29] to further our understanding of the dynamic interactions between pericytes and the endothelium during vessel remodeling and homeostasis, especially with a focus on pericyte migration dynamics and proliferation. Visualization of pericyte behaviors along remodeling microvascular networks will provide new information for understanding the timing, location and activities of pericytes throughout the capillary formation process and guide future investigation of their importance.

In the current study, we utilized two complementary tissue explant models wherein we could observe dynamic vessel

remodeling and associated pericyte behaviors. Specifically, we generated 'double reporter' animals in which pericytes were labeled by *Ng2:DsRed* expression and endothelial cells expressed a *Flk-1:eGFP* reporter gene. To avoid the complication of interpreting the presence of NG2+ oligodendrocyte precursors (OPCs) [38], we selected tissues containing a low to negligible number of these cells. We used time-lapse confocal imaging to examine *ex vivo* (i) adult mesenteric and mesometrium connective tissue undergoing vessel remodeling following exogenous stimulation [37, 39], and (ii) embryonic skin in which new vasculature formed from endogenous genetic and molecular regulation [31]. In both adult and embryonic vascular remodeling settings, we found that a subset of pericytes actively disengaged from the vessel wall. Pericytes adjacent to endothelial sprout initiation sites exhibited a higher rate of filopodial sampling as compared to pericytes at other locations throughout the vascular networks. Similarly, pericytes adjacent to sprouting endothelial cells were more likely to initiate a persistent and directional migration along newly forming vessels. Pericyte proliferation was also more frequent with respect to distinct locations within the remodeling microvasculature, specifically coinciding with elongating endothelial sprouts, which was further supported by *in vivo* observations. Overall, these data demonstrate that pericyte shedding, migration and proliferation are highly integrated with endothelial cell behaviors within actively remodeling capillary beds. Pericyte divestment from the microvessel wall may occur as a necessary physiological process to promote structural plasticity and subsequent outward endothelial cell migration, highlighting a potentially new avenue for further investigation of multicellular remodeling during angiogenic sprouting. These results also highlight that pericytes along capillaries are likely not all phenotypically the same, and their function might depend on their location or subtype. Perhaps more importantly, our findings—made possible by novel time-lapse visualization of pericyte dynamics—motivate new questions related to pericyte cell fate and relationships with interstitial cell types.

MATERIALS AND METHODS

Animal husbandry and genetics

All animal experiments were conducted with review and approval from the Virginia Tech and University of Florida IACUC. All protocols were reviewed and approved by VT and UF IACUC boards. The Virginia Tech NIH/PHS Animal Welfare Assurance Number is A-32081-01 (expires 31 July 2021). Mice expressing enhanced GFP (eGFP) under control of the *Flk-1* (Vascular Endothelial Growth Factor Receptor-2) promoter (i.e. *Flk-1:eGFP* mice) [$Kdr^{tm2.1Jrt/J}$, #017006, The Jackson Laboratory] were set up in timed mating with females expressing the red fluorescent protein variant (DsRed.T1) under control of the mouse NG2 (*Ng2/Cspg4*) promoter/enhancer (i.e. *Ng2:DsRed* mice) [NG2DsRedBAC or Tg(Cspg4-DsRed.T1)1Akik/J, #008241, The Jackson Laboratory] to create 'double reporter' mouse progeny.

Adult mesenteric and mesometrium tissue explant

The oil stimulation protocol to induce vascularization of the mesenteric connective tissue followed previously established methods reported in Suarez-Martinez *et al*. *Microcirc* 2018 [37]. Briefly, adult, female *Flk-1:eGFP*; *Ng2:DsRed* and *Ng2:DsRed* only mice received a single intraperitoneal (IP) injection of 0.1 ml of sterile sunflower oil for five consecutive days. Mesentery tissues from the 'double reporter' mice and mesometrium tissues from *Ng2:DsRed* only mice were harvested 21 or 26 days after the last oil injection, as previously described [37, 39]. Excised tissues were spread on cell-crown inserts with membranes and inverted into 6-well plates with 4 ml of minimum essential medium (Gibco) + 1% penicillin–streptomycin +20% fetal bovine serum (FBS) (see Supplemental Fig. 1). Tissues were incubated under normal culture conditions (37°C, 5% CO_2, humidity) for 5 days, and media was changed every 24 hours.

Embryonic dorsal skin explant

Following mating with double-reporter *Flk-1:eGFP; Ng2:DsRed* males, pregnant c57BL/6 female mice were sacrificed at 14.5 days postcoitum or embryonic day 14.5 (E14.5) by CO_2 inhalation and cervical dislocation. An abdominal incision was made at the midline, and the intestines were moved toward the upper abdomen, exposing the uterus. The uterus was dissected and rinsed in a dish containing cold phosphate buffer saline (PBS). The uterine membrane was dissociated to extract the embryos. Embryos were placed into a separate dish of cold dissection media containing DMEM-H + 5% antibiotic/antimycotic (Gibco) to visually genotype via fluorescence under a dissection microscope. Embryos positive for both *Ng2-DsRed* (i.e. pericyte signal) and *Flk1-eGFP* (i.e. endothelial cell signal) were selected for further microdissection to isolate dorsal skin, again tissue lacking NG2+ OPCs/glia [38]. Embryos were transferred to 35-mm dish with cold dissection media. Dorsal skin was cut along the midline, down the spine to the base of the tail. The skin flap extended outward to the hindlimbs and back around the top of the head. Small forceps placed underneath the dermal tissue were cyclically opened and closed to incrementally dissociate the dermis from the embryo proper while avoiding damaging the sample. Dermal tissues were placed in single wells of a glass-bottom 6-well plate (in-house fabrication) and embedded in a fibrin matrix [40] with the hypodermis (subcutaneous layer) facing the glass. Embryonic skin cultures were allowed to equilibrate for 10 minutes at room temperature, then 20 minutes in a cell culture incubator. Basic culture media (DMEM-H + 10% FBS +5% antibiotic–antimycotic) was added at 3 ml per well.

Live imaging of *ex vivo* angiogenesis in adult mesentery/mesometrium and embryonic skin

Adult mesentery and embryonic tissue culture plates were transferred to an incubation chamber (37°C, 5% CO_2, humidity controlled) mounted on a Zeiss LSM880 confocal microscope (Carl Zeiss, Thornwood, NY, USA) for live imaging [31]. Multiposition, time-lapse confocal scans were acquired through each sample thickness (z-stacks: 6–15 images with 1–2 microns between planes) at 20–25 minute intervals for a minimum of 12 hours using a 20× objective. Through-thickness z-stacks at each time point were compressed (maximum intensity projections) and exported as a video file (TIF stack or AVI) in RGB channel format. Representative movie sequences shown are from nonconsecutive images.

Adult mesometrium tissue culture plates were also transferred to an incubation chamber (37°C, 5% CO2, humidity controlled) mounted on a Nikon Eclipse Ti2 inverted fluorescent microscope (Nikon, Melville, NY, USA) for live imaging. Time-lapse imaging of NG2+ cells at certain locations was acquired for 144 hours using a 10× objective. On Day 0, images were taken every 12 hours, Day 1–3 images were taken every 2 hours, and Day 4 and 5 images were taken every 4 hours. Images were compiled

into a TIF stack using ImageJ and then converted into an AVI file to create the movies.

Quantitative movie analysis—adult mesometrium

Live imaging analysis of adult mesometrium vessel formation included tracking movements of individual NG2+ cells from *Ng2:DsRed* only mice to identify distinct cell behaviors. Four unique dynamics emerged: (i) NG2+ pericytes migrating from vessel networks into the interstitial space, (ii) NG2+ cells migrating from the interstitial space onto microvessels, (iii) NG2+ pericytes that migrated from one location within the microvasculature to another part of the network and (iv) NG2+ pericytes along microvessels that were stationary, exhibiting no movement. Each movie was analyzed multiple times to track individual NG2+ cells that moved within the tissue, assigning it to one of the four categories described above. The number of cells that clearly exhibited one of the four behaviors was quantified for each movie ($n = 4$ movies of mesometrium tissues from two different animals). A subset of NG2+ cells were excluded from quantification due temporal gaps in imaging, cell movement beyond the region-of-interest, and loss of distinct signal, among other minor technical issues.

Quantitative movie analysis—embryonic skin

Movies of *ex vivo* blood-vessel development in E14.5 dorsal skin explants were first analyzed using FIJI/ImageJ for endogenous pericyte distribution along the vasculature ($n = 4$ movies of embryonic dorsal skin explants from four different animals). Initial pericyte distribution was established by identifying NG2+ cells on microvessels at the following morphological locations: (i) established vessel lengths, (ii) extended endothelial sprouts, (iii) at a vessel branch point and (iv) at the base of sprouting endothelial cell (see Supplemental Fig. 1). The percent of pericytes at each location was calculated as the number of pericytes at a given locale over the total number of discernable pericytes within the region of vasculature imaged. Vessel-remodeling activity was observed over the entire imaging time-course. From these temporal data and vessel morphology, distinct network regions were classified into subtypes of remodeling activity, as done previously [1, 41], specifically: (i) endothelial sprout initiation, (ii) sprout elongation, (iii) vessel connection/anastomosis, (iv) branch point collapse, (v) vessel diameter expansion and (vi) minimal vessel remodeling. All movies were also analyzed for the four behaviors observed in the adult mesometrium tissues as described above.

Pericyte filopodial extensions were analyzed with respect to these specific vessel-remodeling behaviors. Filopodial 'sampling' activity was classified as either 'High' (3+ distinct filopodia) or 'Minimal' (0–2 filopodia). Pericytes were quantified relative to each vessel-remodeling activity and categorized based on filopodial extensions, yielding a percentage of NG2+ pericytes as highly or minimally active in filopodial sampling. Similarly, NG2+ pericyte migration was classified as 'Highly Migratory' or 'Minimally Migratory' based on the total distance traveled, and each pericyte was assigned a location based on nearby vessel-remodeling activity. Pericyte migration was further classified as being highly or minimally directional, i.e. migration in a persistent direction (e.g. along a sprouting vessel) vs. movement lacking sustained directionality. NG2+ pericyte proliferation was also analyzed with respect to vessel remodeling behaviors, yielding percentages of dividing cells in relation to these activities.

Immunostaining, imaging and analysis—postnatal mouse brain vasculature

Wild-type postnatal Day 1 (P1) mice were euthanized by isoflurane overexposure, in accordance with IACUC guidelines. Following a secondary method of euthanasia, animals were perfusion fixed with 4% paraformaldehyde (PFA) via intracardiac infusion (5 ml). The brain was dissected from the skull and immersion fixed in 4% PFA overnight at 4°C. Fixed WT P1 brains were washed in PBS, and prepared for slicing by vibratome. Slices of 100–200 μm in thickness were obtained, placed in single wells of a 24-well plate for antibody immunostaining. Samples were incubated for 30 minutes at room temperature in PBS + 0.1% Triton-X (PBS-T) + 5% normal donkey serum. Primary antibodies were diluted in PBS-T and incubated with slices overnight at 4°C with slight agitation. Secondary antibodies in PBS-T were incubated at room temperature for 1–3 hours with slight agitation. PBS washes (three times for 10 minutes each) occurred in between each step. Primary and secondary antibody combinations included: (i) goat antimouse platelet–endothelial cell adhesion molecule-1 (PECAM-1/CD31, R&D Systems) + donkey antigoat Alexa Fluor® 488 (Jackson ImmunoResearch), (ii) rat antimouse PDGF receptor-β (PDGFRβ/CD140b, clone APB5, ThermoFisher Scientific) + donkey antirat DyLight® 550 (cross-adsorbed, Invitrogen) and (iii) Alexa Fluor® 647 rabbit antimouse phospho-histone H3 (Ser10, clone D2C8, cell signaling). DAPI (4,6-diamidino-2-phenylindole) was applied at 1:1000 for 30 minutes at room temperature to label cell nuclei. Through-thickness images (z-stacks) were acquired on a Zeiss LSM880 confocal microscope, and compressed using FIJI/ImageJ software. Pericytes positive for PDGFRβ and PH3 ($n = 18$ within seven brain slices acquired from two different WT c57BL/6 P1 mice) were scored for their position along vessels based on hallmarks of vessel-remodeling activity (i.e. filopodia for sprouting endothelial tip cells, etc.), vessel diameter expansion, or the lack of obvious endothelial cell rearrangement (i.e. seemingly quiescent).

Statistical analysis

Using GraphPad Prism 8 software, statistical analysis was applied as appropriate. For adult mesometrium data, a one-way Analysis of Variance (ANOVA) test followed by Tukey's multiple comparisons test was used to analyze the differences between the four dynamics; statistical significance was achieved when $P < 0.05$. Pericyte distribution measurements, pericyte filopodial sampling and migration, and pericyte proliferation percentages from live imaging observations and from immunostained brain slices were compared by chi-square analysis; statistical significance was achieved when $P < 0.05$.

RESULTS

Pericytes divest from adult and embryonic capillaries during angiogenic remodeling

Pericytes have often been characterized as 'bumps-on-a-log' [12, 42], suggesting a predilection for associating with capillary segments, though pericytes localizing predominantly to microvessel branch points has also been described [33]. As a singular protein marker for pericytes remains elusive, a combinatorial approach of marker expression and phenotypic characteristics, including morphology and proximity to the endothelium, is required for identification [12, 43].

In this study, we used the pericyte marker *Ng2/Cspg4* to drive DsRed fluorescence, which can also be expressed by OPCs [38] and possibly macrophages [44, 45]. To support the identity of *Ng2:DsRed* + cells as pericytes, we selected a tissue (skin) in which OPCs are sparse if not altogether absent. Additionally, we labeled embryonic skin of *Ng2:DsRed* E14.5 mice with an endothelial cell marker (PECAM-1/CD31) and a macrophage marker (F4/80), finding little to no overlap between the *Ng2:DsRed* and F4/80 signals (Supplemental Fig. 1). Therefore, we began our analysis by establishing a baseline distribution of pericytes throughout vascular networks in embryonic skin before the observed time-course of vascular remodeling. Although there was a slight increase in the percentage of *Ng2:DsRed* + cells at vessel branch points, pericytes were mostly distributed evenly across vessel lengths and branch points, along extended endothelial cell sprouts, and at the base of sprouting vessels (Supplemental Fig. 2). Establishing pericyte distribution throughout the network was important for subsequent interpretation of pericyte activity, as their initial location within the microvasculature may correlate to their dynamics during vessel remodeling. For example, finding a higher density of pericytes at a specific location might suggest an increase in particular actions such as dividing or migrating.

To address the frequency of distinct pericyte behaviors, we began by assessing pericyte movements within the adult mesenteric and mesometrium vascular networks as well as in the embryonic dorsal skin vasculature. We hypothesized that a large wave of pericyte detachment might occur during the initial stages of vascular remodeling to allow greater endothelial cell plasticity in sprouting and outward migration [15–17]. We found that, from both adult and embryonic capillaries, pericyte divestment occurred, seemingly as a phase of 'pericyte shedding' (Fig. 1 and Supplemental Movies 1 and 2); however, more studies will be necessary to determine if this phenomenon directly facilitates angiogenic remodeling or occurs for other purposes. Nevertheless, the majority of pericytes in the mesometrium (~70%) and embryonic skin (~80%) remained on microvessels (Fig. 1B and D). This observation is consistent with the well-established role of pericytes in maintaining vessel stability [9–11]. Embryonic pericytes also remained in relatively fixed positions unless an angiogenic event occurred in close proximity. While pericytes migrating into the interstitial space were tracked for the duration of each live imaging session, we were unable to assign any new discrete cell behaviors that might suggest a new physiologic role. Consequently, our observations of pericyte shedding introduce new and intriguing questions regarding (i) mechanisms that drive detachment at specific locations, (ii) cell population distinctions and (iii) the ultimate cell fate for disengaged pericytes migrating into the interstitium [22, 46, 47], among others, all of which warrant further investigation.

Although the angiogenic activity was relatively comparable between the adult and embryonic tissue explant models, the rate of structural remodeling was generally higher in the embryonic tissue; we therefore focused the remainder of the study on the embryonic dorsal skin explant model for experimental tractability. We also concentrated the remainder of our analysis on the subpopulation of pericytes that remained physically associated with the vasculature.

Pericyte filopodial sampling and migration activity increase near endothelial sprout initiation sites

Berthiaume *et al*. recently observed pericytes extending cellular processes akin to filopodia to re-establish coverage of brain microvessels from which a pericyte had been removed by laser ablation [27]. The authors did not observe the migration of adjacent pericytes into these regions, suggesting the presence of a cue sufficient to stimulate filopodial extension but not to induce cell migration. Within an actively remodeling vascular network, it is plausible that pericyte filopodial 'sampling' of their local microenvironment would dramatically increase in response to the regional abundance of proangiogenic cues, such as those generated at the angiogenic sprouting front [6]. Interestingly, quantification of live confocal imaging in our embryonic skin explant model we found that pericytes adjacent to endothelial cells undergoing sprout initiation as 'tip' cells [4–7] were more likely to exhibit a high level of filopodial extension and retraction i.e. sampling (Fig. 2 and Supplemental Movie 3). These observations are consistent with data suggesting high secretion levels of pericyte-recruiting factor, PDGF-BB [48], from endothelial tip cells during the onset of angiogenesis [6, 48, 49], although additional studies are needed to establish the underlying molecular mechanisms. In contrast, pericytes in other regions of the vasculature, particularly on elongating vessel sprouts, displayed very little filopodia activity (Fig. 2 and Supplemental Movie 3).

We complemented our analysis of pericyte filopodia dynamics with quantification of directional pericyte migration along microvessels. We reasoned that perhaps the lower levels of pericyte filopodia sampling on elongating sprouts was due, in part, to a shift toward a more migratory phenotype for pericytes near sprouting endothelial cells. We found that pericytes were not uniformly migratory within the vasculature, as pericytes were not highly migratory on relatively quiescent vessels or on vessels experiencing diameter expansion or branch point collapse [1] (Fig. 3 and Supplemental Movie 4). Pericytes were notably more migratory on vessels undergoing sprout initiation, elongation and connection, with pericytes adjacent to sprout initiations showing a significant increase in migratory behavior. In addition, pericytes near sprout initiation sites were significantly more directional in their migration, that is, they persisted in a uniform direction more often (largely in the direction of a lengthening sprout) (Fig. 3 and Supplemental Movie 4). Highly migratory pericytes on elongating and connecting sprouts displayed less directional migration, as their movements were seemingly more randomized and not sustained in a particular direction. Thus, chemotactic cues from sprouting endothelial cells seem to induce a phenotypic transition for pericytes to shift from being largely stationary to more migratory. This transition appears to entail an initial phase of active filopodial sampling and then a subsequent progression to directional migration to maintain pericyte coverage of nascent vessel sprouts.

Pericyte divisions occur predominantly along elongating angiogenic sprouts

Sprouting endothelial cells secrete high levels of PDGF-BB [6, 48, 49], which is a potent mitogen for microvascular pericytes [49, 50]. We hypothesized that, given the increase in filopodial and migratory activity of pericytes near endothelial sprout initiation sites, pericyte proliferation would also be more frequent at these locations. Although *Ng2:DsRed* + pericytes divided at sprout initiations sites and at connection points with a moderate level of frequency, the majority of pericyte divisions occurred adjacent to elongating endothelial cell sprouts (Fig. 4 and Supplemental Movie 5). In several cases, multiple pericyte divisions were observed along the same sprout. However, the mechanisms driving these phenomena remain unclear, with possibilities including, but not limited to, PDGF-BB signaling

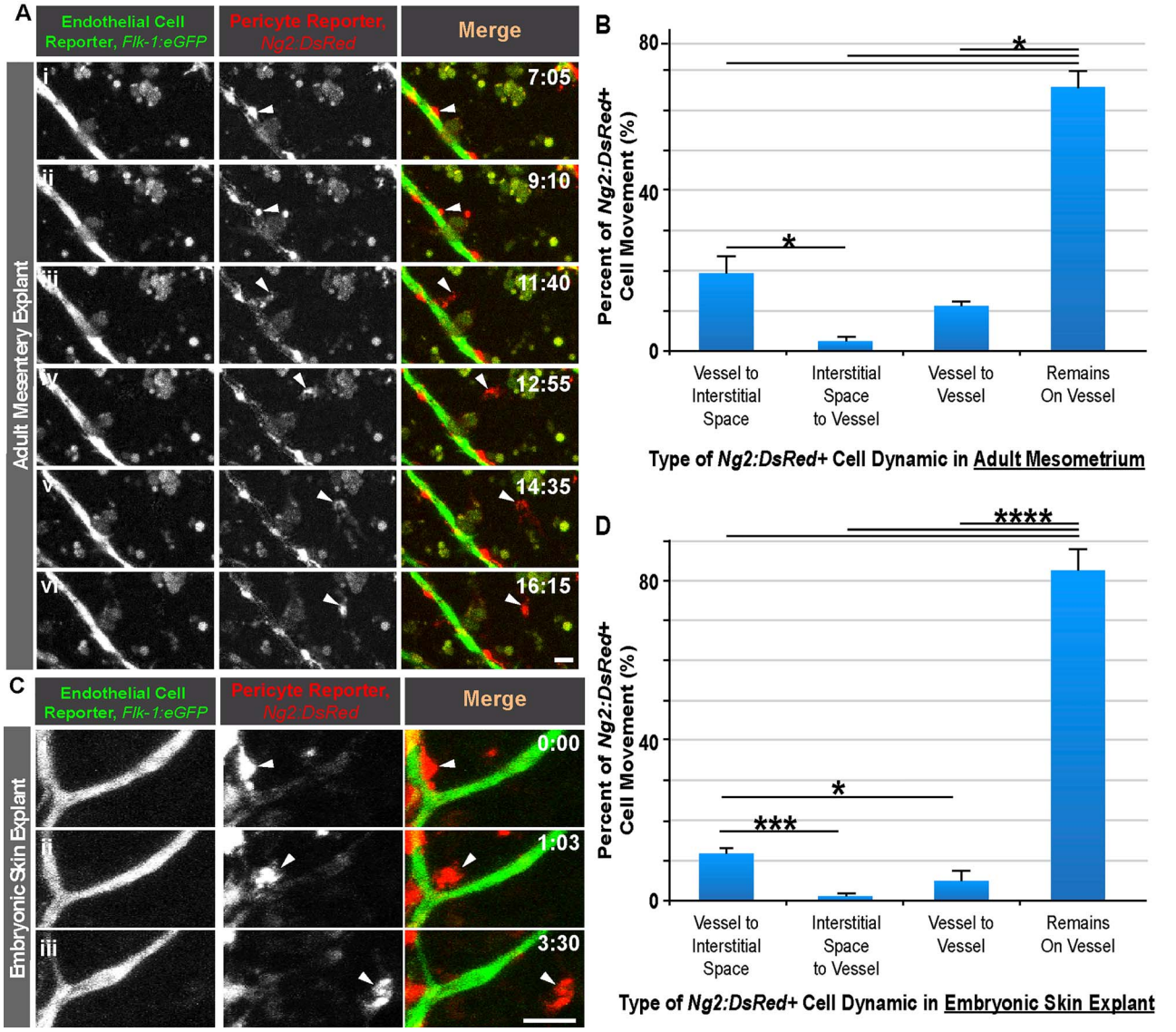

Figure 1. Pericyte shedding during angiogenic sprouting of adult and embryonic microvessels. (A): Time-lapse images of *Flk-1:eGFP*+ endothelial cells (i-vi, left-most column, and green in right-most column) and *Ng2:DsRed* + vascular pericytes (i-vi, middle column, and red in right-most column) during pericyte detachment (arrowhead) in an adult mesentery explant model. Scale bar, 20 μm. Time (hh:mm), upper right. 'Full movie from which nonconsecutive stills were selected, Supplemental Movie 1.' (B): Percent of *Ng2:DsRed* + cell movement for each type of dynamic in an adult mesometrium explant model. Data were quantified from four biological replicates of distinct movies. *$P < 0.05$ by ANOVA followed by Tukey's multiple comparisons test. Error bars, SEM. (C): Time-lapse images of *Flk-1:eGFP*+ endothelial cells (i-iii, left-most column, and green in right-most column) and *Ng2:DsRed* + vascular pericytes (i-iii, middle column, and red in right-most column) during pericyte detachment (arrowhead) in an embryonic skin explant model. Scale bar, 20 μm. Time (hh:mm), upper right. 'Full movie from which nonconsecutive stills were selected, Supp. Movie 2.' (D): Percent of *Ng2:DsRed* + cell movement for each type of dynamic in an embryonic dorsal skin explant model. Data were quantified from four biological replicates of distinct movies. *$P < 0.05$, ***$P < 0.005$, ****$P < 0.001$ by ANOVA followed by Tukey's multiple comparisons test. Error bars, SEM.

[48], morphological geometry [51, 52], mechanical environment [53], and ECM substrate [54].

To further support these live imaging data, we collected tissues undergoing substantial vascular growth and development in the early postnatal stages, specifically from the P1 mouse brain. We targeted our analysis to a region containing rapidly proliferating glial and neuronal precursors [9, 25], which creates hypoxic conditions that fuel robust angiogenic growth including pericyte proliferation. This area is located approximately within the caudothalamic groove, residing posterior to the intraventricular foramen, in the floor of the lateral ventricle. Brain slices were immunolabeled for mitotic cells with an antibody against phospho-histone H3 (PH3) [55, 56] and costained for endothelial cells (i.e. platelet–endothelial cell adhesion molecule-1, PECAM-1/CD31) and pericytes (i.e. PDGF Receptor-β, PDGFRβ/CD140b). Confocal imaging and quantitative analysis of these *in vivo* preparations corroborated the dynamic imaging of pericyte divisions *ex vivo*, providing evidence of mitotic pericytes within actively angiogenic regions, particularly on elongating endothelial cell sprouts (Fig. 5). Observations from both experimental approaches support the idea that endothelial sprouts extending from a parent vessel provide a more favorable, though not exclusive, configuration for promoting pericyte proliferation in developing vascular networks.

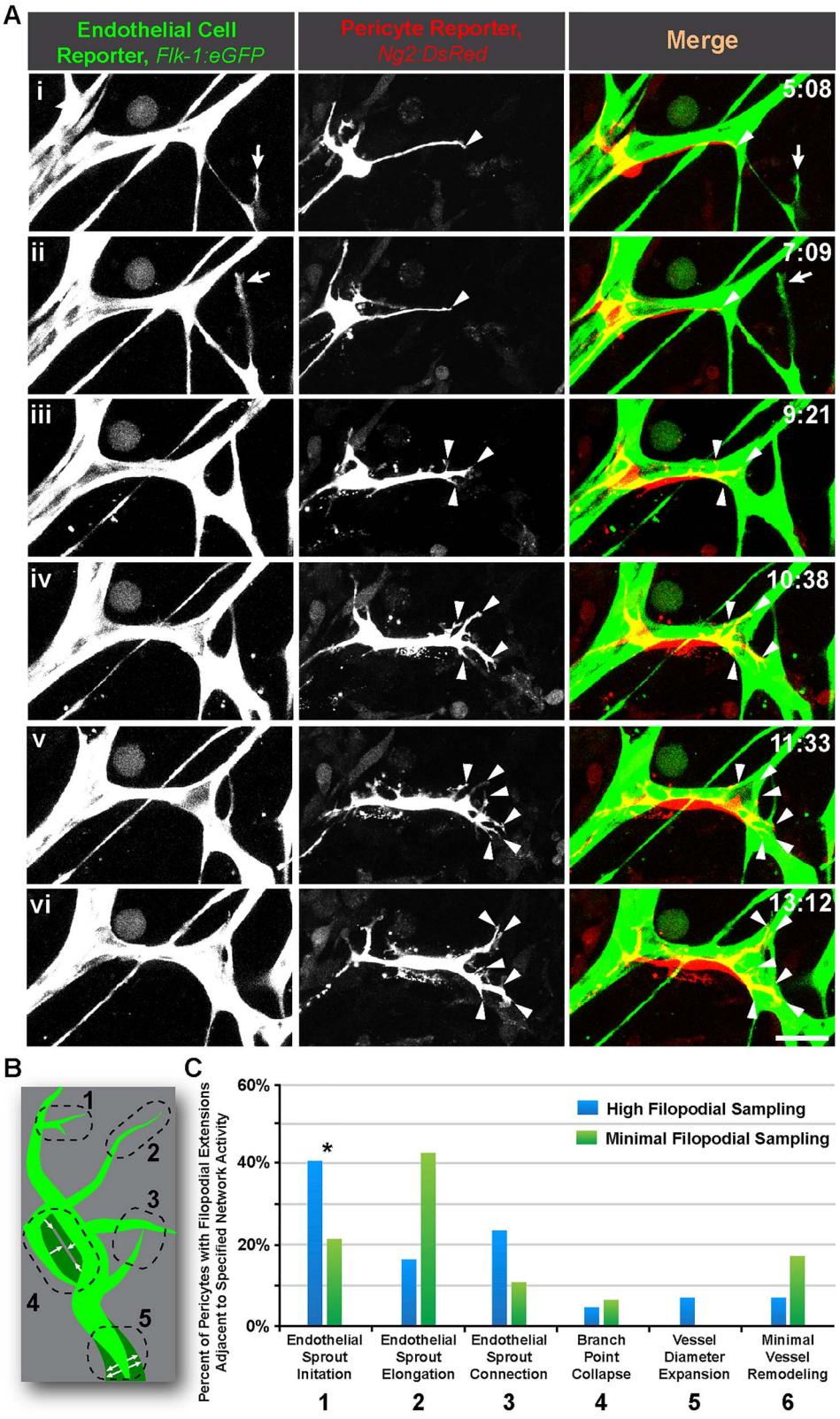

Figure 2. Pericyte filopodial sampling is most active near locations of endothelial sprout initiation. (A): Time-lapse images of *Flk-1:eGFP*+ endothelial cells (i-iii, left-most column, and green in right-most column) and *Ng2:DsRed* + vascular pericytes (i-iii, middle column, and red in right-most column) during endothelial sprout initiation (arrow) and pericyte filopodial sampling (arrowheads) in an embryonic skin explant model. Scale bar, 20 μm. Time (hh:mm), upper right. 'Full movie from which nonconsecutive stills were selected, Supplemental Movie 3.' (B): Schematic illustrating five distinct regions of the vasculature (green) undergoing different remodeling behaviors with each number corresponding to the descriptions in (C). See Chappell *et al.* [1] for additional visual examples of regions. (C): Percent of *Ng2:DsRed* + pericytes with detectable filopodial extensions located adjacent to the specific network activity (i.e. remodeling behavior). Blue bars represent high filopodial sampling (3+ extensions), and green bars represent minimal filopodial sampling (two or fewer extensions). Data were quantified from four biological replicates of distinct movies (pooled), with each sprout as single technical event. Specific fields of view were localized to the angiogenic (sprouting) front within the embryonic dorsal skin explant. *$P < 0.05$ by chi-square analysis.

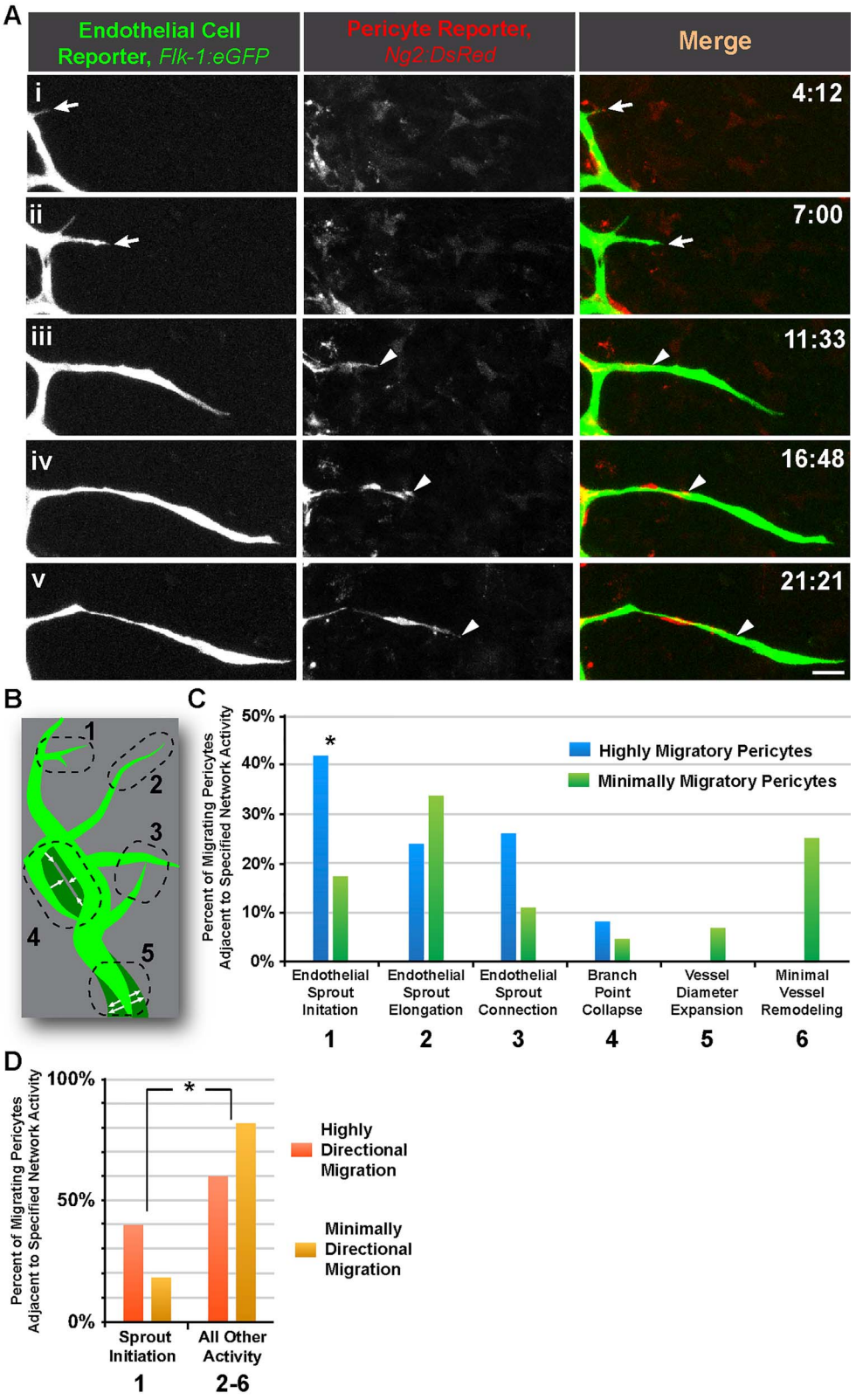

Figure 3. Pericyte migratory behavior is elevated and more directional adjacent to endothelial sprout initiation sites. (A): Time-lapse images of *Flk-1:eGFP*+ endothelial cells (i-v, left-most column, and green in right-most column) and *Ng2:DsRed* + vascular pericytes (i-v, middle column, and red in right-most column) during endothelial sprout initiation (arrow) and elongation, and pericyte migration (arrowheads) in an embryonic skin explant model. Scale bar, 20 μm. Time (hh:mm), upper right. 'Full movie from which nonconsecutive stills were selected, Supplemental Movie 4.' (B): Schematic illustrating five distinct regions of the vasculature (green) undergoing different remodeling behaviors with each number corresponding to the descriptions in (C). See Chappell *et al.* [1] for additional visual examples of regions. (C): Percent of migrating *Ng2:DsRed* + pericytes located adjacent to the specific network activity (i.e. remodeling behavior). Blue bars represent highly migratory pericytes, and green bars represent minimally migratory pericytes. Data were quantified from four biological replicates of distinct movies (pooled), with each sprout as single technical event. Fields of view were localized to the angiogenic (sprouting) front within the embryonic dorsal skin explant. $^{*}P < 0.05$ by chi-square analysis. (D): Percent of migrating *Ng2:DsRed* + pericytes located adjacent to the specific network activity (i.e. remodeling behavior), 1 vs. 2–6 in (C). Orange bars represent highly directional migration, and yellow bars represent minimally directional migration. $^{*}P < 0.05$ by chi-square analysis.

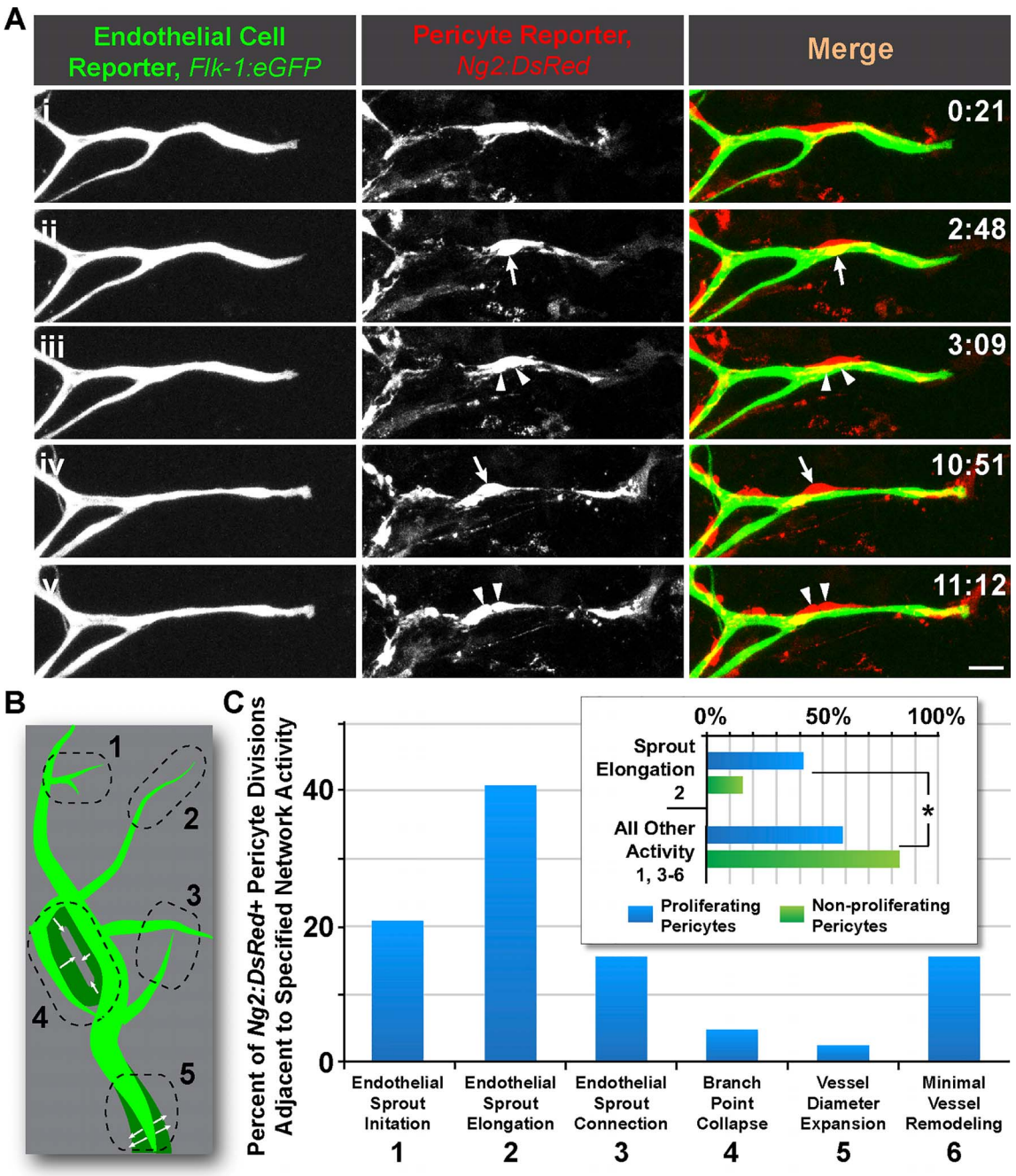

Figure 4. Pericyte proliferation occurs most frequently along elongating endothelial sprouts in embryonic skin microvascular networks. (A): Time-lapse images of *Flk-1:eGFP*+ endothelial cells (i-v, left-most column, and green in right-most column) and *Ng2:DsRed* + vascular pericytes (i-v, middle column, and red in right-most column) during endothelial sprout elongation and pericyte division (arrows then associated arrowheads) in an embryonic skin explant model. Scale bar, 20 μm. Time (hh:mm), upper right. 'Full movie from which nonconsecutive stills were selected, Supplemental Movie 5.' (B): Schematic illustrating five distinct regions of the vasculature (green) undergoing different remodeling behaviors with each number corresponding to the descriptions in (C). See Chappell *et al.* [1] for additional visual examples of regions. (C): Percent of *Ng2:DsRed* + pericyte divisions located adjacent to the specific network activity (i.e. remodeling behavior). Blue bars represent percentages of all pericyte divisions observed. Inset graph: Percent of *Ng2:DsRed* + pericytes located adjacent to the specific network activity (i.e. remodeling behavior), 2 vs. 1, 3–6 in (C). Blue bars represent proliferating pericytes, and green bars represent nonproliferative pericytes. Data were quantified from four biological replicates of distinct movies (pooled), with each sprout as single technical event. Fields of view were localized to the angiogenic (sprouting) front within the embryonic dorsal skin explant. *$P < 0.05$ by chi-square analysis.

DISCUSSION

Pericytes play key roles in stabilizing the microcirculation following vessel remodeling [9–11], in addition to other essential functions [12]. Their proximity to endothelial cells during angiogenesis [13, 14] suggests an important crosstalk between these two cell types at various stages in this process. As insight into the cellular and molecular mechanisms coordinating their interactions continues to grow, it appears increasingly likely

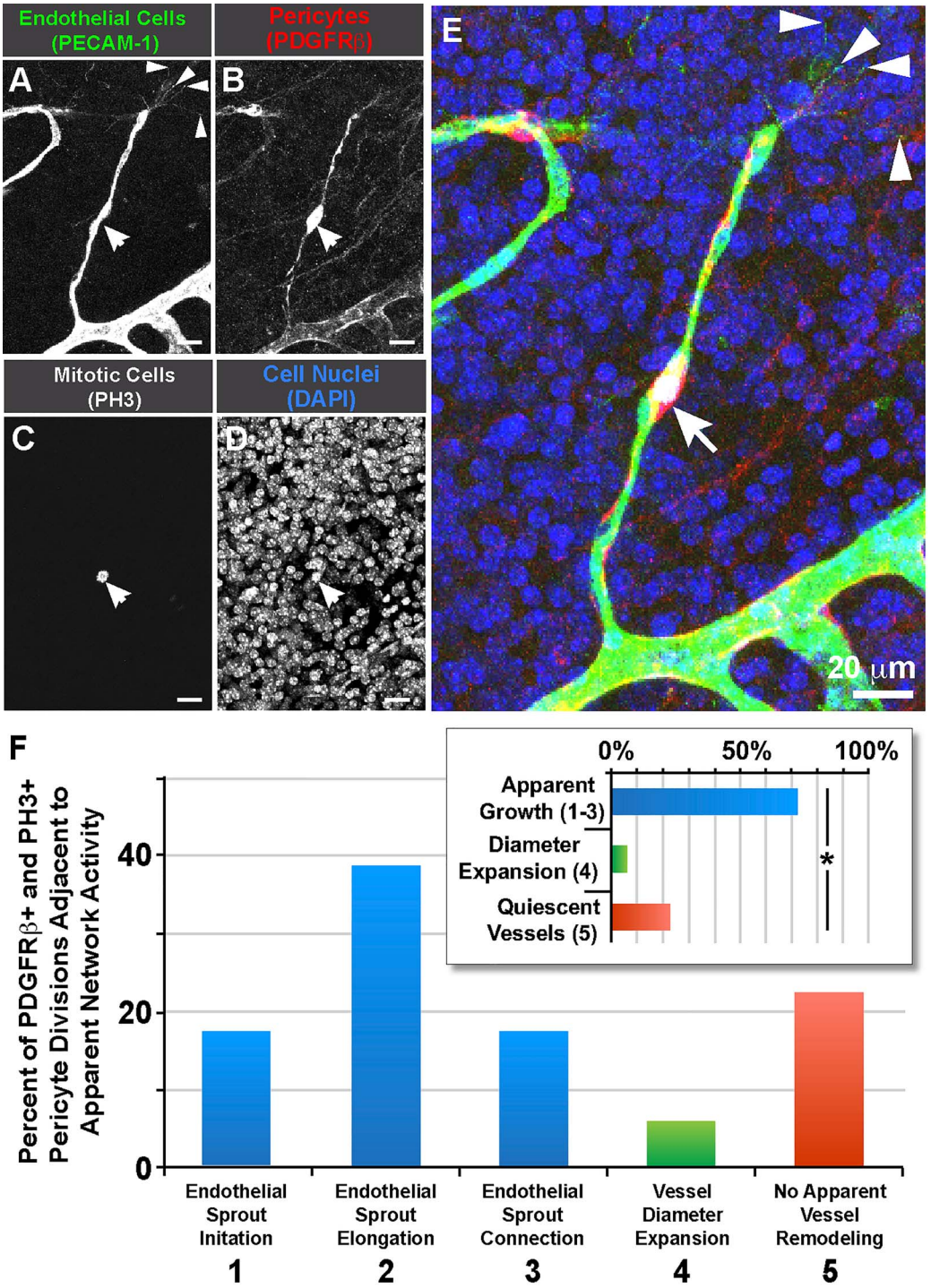

Figure 5. Pericyte divisions occur along endothelial sprouts in postnatal brain capillaries within the caudothalamic groove. (A): Endothelial cells labeled for PECAM-1 (green in E). (B): Vascular pericytes labeled for PDGFRβ (red in E). (C): Mitotic cell labeled for phospho-histone H3 (white in E, arrow). (D): Cell nuclei labeled by DAPI (blue in E). (E): Merged image of all signals. Endothelial 'tip' cell filopodia denoted with arrowheads. Scale bar, 20 μm. (F): Percent of PDGFRβ+ pericyte divisions (PH3+) located adjacent to the apparent network activity (i.e. remodeling behavior). Blue bars represent percentages of all pericyte divisions observed in regions exhibiting vessel growth behaviors (i.e. sprout initiation, elongation and connection), green bars represent percentages of pericyte divisions occurring in vessels undergoing diameter expansion, and red bars represent percentages of pericyte divisions within seemingly quiescent vessels. Inset graph: Percent of PDGFRβ+ pericytes located adjacent to the specific network activity i.e. 1–3 (blue bar) vs. 4 (green bar) vs. 5 (red bar). Data were quantified from seven distinct brain slices from two WT brains (pooled), with each pericyte as single technical event ($n = 18$). $^{*}P < 0.05$ by chi-square analysis.

that phenotypically distinct subpopulations of pericytes exist during capillary sprouting [57–60]. In this study, we applied live imaging approaches to adult and embryonic tissue explant models of angiogenic remodeling, facilitating classification of endothelial cells and pericytes engaged in distinct cellular behaviors (Fig. 6). Consistent with previous observations from

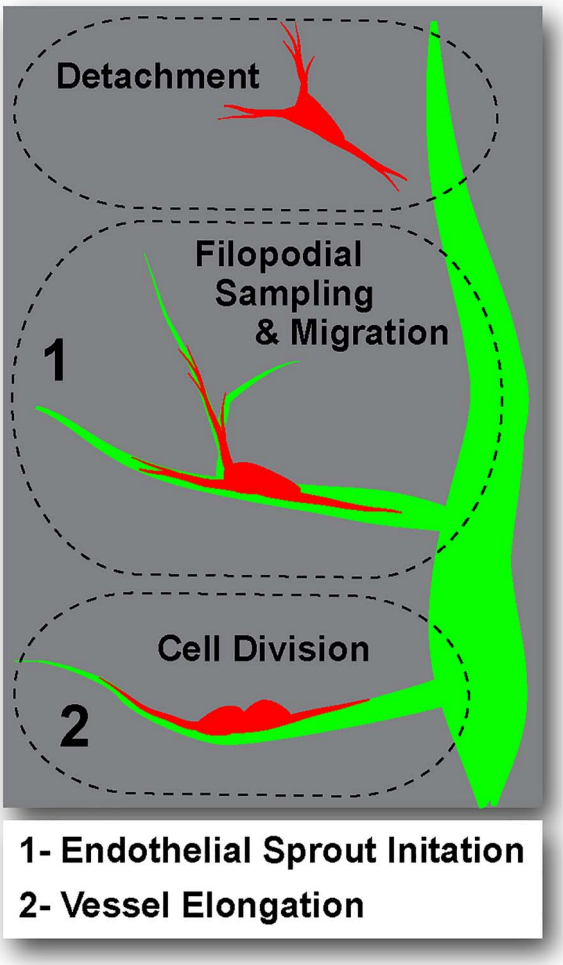

Figure 6. Schematic illustrating phenotypically distinct pericyte subpopulations. Pericyte (red) behaviors relative to the endothelium (green) included: detachment or 'shedding' from the vessel wall (upper dashed oval), filopodial sampling and migration near endothelial sprout initiation sites (region 1, middle dashed oval), and cell division on elongating vessels (region 2, lower dashed oval).

a variety of models [20–22], we observed numerous instances of pericyte detachment from the microvessel wall. Although further investigation is needed, it is possible that this phase of 'pericyte shedding' enables disassembly of the vessel wall to allow greater plasticity for endothelial cell remodeling including angiogenic sprouting [15–17]. Vessel-associated pericytes adjacent to endothelial cells initiating new vessel sprouts demonstrated a high level of filopodial sampling of their local microenvironment as well as increased directional migration, largely along angiogenic sprouts. Further evidence of tight synchronization between endothelial cell and pericyte behaviors was found in the elevated frequency of pericyte divisions on elongating endothelial cell sprouts. Thus, similar to the phenotypic diversity of endothelial subtypes observed during angiogenesis (i.e. tip vs. stalk vs. phalanx cells) [2, 61–63], pericytes may also assume distinct functional roles according to their location and/or subtype, which appears to be highly integrated with endothelial cell activity and behaviors.

Pericyte detachment from the capillary wall has primarily been associated with microvascular dysfunction in certain disease states such as proliferative diabetic retinopathy [20], idiopathic pulmonary fibrosis [21] and kidney disease [22], among others. Pericyte loss or absence from the vessel wall has also been described as a hallmark of the progression of many solid tumor types [64]. We found that, in both embryonic and adult tissues undergoing active vascular remodeling, pericytes appeared to 'shed' from the vessel wall. Although we did not measure pericyte divestment from the microvasculature in direct relation to subsequent angiogenic sprouting in this study, it is interesting to consider that outward pericyte migration could be a component of the coordinated disassembly of blood vessels that must occur before extensive structural remodeling can proceed [15–17], suggesting new dynamics for further investigation. Our analysis was also unable to identify a definitive transformation of dissociated pericytes into other unique cell types, although such a transition has been described for pericytes in becoming myo−/fibroblasts or perhaps a cell type very similar to these interstitial cells [21, 65, 66]. Not all pericytes observed in our embryonic and adult models detached from microvessel. Discrete subpopulations of vessel-associated pericytes engaged in active migration and coordinated cell division, and many others remained stationary and integrated within the vessel wall. This phenotypic diversity aligns with a similar heterogeneity found in pericyte marker expression [57–60] and morphology [27] at distinct locations throughout the microcirculation. Overall, our study reinforces the notion that, similar to the phenotypic specification of endothelial cells during angiogenesis [2, 61–63], pericytes may also assume distinct roles and subtypes to support the various stages of vessel remodeling [1]. Pericytes may also adopt these unique roles to maintain a level of vessel coverage so they can quickly transition into promoting vascular stabilization and quiescence as angiogenesis concludes.

Although we initially expected pericytes to divide more frequently near endothelial cells undergoing sprout initiation, pericyte mitosis occurred most often along endothelial sprouts that were extending from the parent vessel. This observation is consistent with previous studies suggesting that a linear orientation is more favorable for cell division [51, 52]. It is possible that cellular geometry, PDGF-BB retained along the vessel wall, and local ECM composition collectively contribute to this promitotic environment for pericytes [54], and warrants further investigation. For instance, there is likely to be regional heterogeneity in the ECM components of the vBM that contribute mechanistically to the diverse functions of pericyte subtypes during angiogenesis. Endothelial cells and pericytes may collaborate to build this provisional vBM during angiogenic sprouting to stimulate and support pericyte proliferation, expansion and subsequent investment into new vessel branches.

The dynamic crosstalk between pericytes and endothelial cells during microvascular remodeling necessitates the development of new models and approaches to capture and compare their interactions in a variety of settings [67]. For example, in the present study, we found that adult blood vessels undergo pericyte detachment in a manner consistent with embryonic vasculature, suggesting this phenomenon may be conserved from early vascular development and re-engaged during adult angiogenesis. Taking into consideration that our observations were quantified in models that are devoid of key physiological inputs such as blood flow and immune cell recruitment, the coupling our findings with corresponding *in vivo* scenarios will further expand our understanding of their physiological relevance. Pericytes are known to disengage from the vessel wall *in vivo* [21, 22], for instance, and the models presented here can begin to address questions surrounding their detachment—does

pericyte shedding immediately precede angiogenic activity? How do pericytes redistribute after detachment? Do they reassociate with endothelial sprouts to promote stabilization? Observations from these models might also guide development of clinical therapies seeking to restore pericyte coverage [20, 33–35], as pericyte proliferation and migration along the microvascular endothelium may only occur at substantial levels during angiogenic stimulation and subsequent vessel remodeling.

DISCLOSURES

None.

ABBREVIATIONS

ECM, extracellular matrix; platelet-derived growth factor receptor-β, PDGFRβ; NG2, neural glial antigen-2; vBM, vascular basement membrane; Col-IV, type IV Collagen; VEGF-A, vascular endothelial growth factor-A.

ACKNOWLEDGEMENTS

We thank the Chappell and Murfee labs for critical and extensive discussions of the primary data, and the Kushner lab for technical expertise provided.

FUNDING

This work was supported in part by funding from the National Institutes of Health (R01-HL146596 to J.C.C. and R01-AG049821 to W.L.M.) and the National Science Foundation (CAREER Award 1752339 to J.C.C.).

SUPPLEMENTARY DATA

Supplementary data is available at *INTBIO Journal* online.

CONFLICT OF INTEREST STATEMENT

None declared.

REFERENCES

1. Chappell JC, Cluceru JG, Nesmith JE et al. Flt-1 (VEGFR-1) coordinates discrete stages of blood vessel formation. *Cardiovasc Res* 2016;**111**:84–93.
2. Jakobsson L, Franco CA, Bentley K et al. Endothelial cells dynamically compete for the tip cell position during angiogenic sprouting. *Nat Cell Biol* 2010;**12**:943–53.
3. Tirziu D, Simons M. Endothelium as master regulator of organ development and growth. *Vascul Pharmacol* 2009; **50**:1–7.
4. Peirce SM, Mac Gabhann F, Bautch VL. Integration of experimental and computational approaches to sprouting angiogenesis. *Curr Opin Hematol* 2012;**19**:184–91.
5. Bentley K, Mariggi G, Gerhardt H et al. Tipping the balance: Robustness of tip cell selection, migration and fusion in angiogenesis. *PLoS Comput Biol* 2009;**5**:e1000549.
6. Hellstrom M, Phng LK, Hofmann JJ et al. Dll4 signalling through Notch1 regulates formation of tip cells during angiogenesis. *Nature* 2007;**445**:776–80.
7. Gerhardt H, Golding M, Fruttiger M et al. VEGF guides angiogenic sprouting utilizing endothelial tip cell filopodia. *J Cell Biol* 2003;**161**:1163–77.
8. Bentley K, Franco CA, Philippides A et al. The role of differential VE-cadherin dynamics in cell rearrangement during angiogenesis. *Nat Cell Biol* 2014;**16**:309–21.
9. Braun A, Xu H, Hu F et al. Paucity of pericytes in germinal matrix vasculature of premature infants. *J Neurosci* 2007;**27**:12012–24.
10. von Tell D, Armulik A, Betsholtz C. Pericytes and vascular stability. *Exp Cell Res* 2006;**312**:623–9.
11. Lindahl P, Johansson BR, Leveen P et al. Pericyte loss and microaneurysm formation in PDGF-B-deficient mice. *Science* 1997;**277**:242–5.
12. Armulik A, Genove G, Betsholtz C. Pericytes: Developmental, physiological, and pathological perspectives, problems, and promises. *Dev Cell* 2011;**21**:193–215.
13. Payne LB, Zhao H, James CC et al. The pericyte microenvironment during vascular development. *Microcirculation* 2019;**26**:e12554.
14. Walpole J, Gabhann FM, Peirce SM et al. Agent-based computational model of retinal angiogenesis simulates microvascular network morphology as a function of pericyte coverage. *Microcirculation* 2017;**24**:1–14.
15. Funahashi Y, Shawber CJ, Sharma A et al. Notch modulates VEGF action in endothelial cells by inducing matrix Metalloprotease activity. *Vasc Cell* 2011;**3**:2.
16. Virgintino D, Girolamo F, Errede M et al. An intimate interplay between precocious, migrating pericytes and endothelial cells governs human fetal brain angiogenesis. *Angiogenesis* 2007;**10**:35–45.
17. Davis GE, Saunders WB. Molecular balance of capillary tube formation versus regression in wound repair: Role of matrix metalloproteinases and their inhibitors. *J Investig Dermatol Symp Proc* 2006;**11**:44–56.
18. Potente M, Gerhardt H, Carmeliet P. Basic and therapeutic aspects of angiogenesis. *Cell* 2011;**146**:873–87.
19. Ridgway J, Zhang G, Wu Y et al. Inhibition of Dll4 signalling inhibits tumour growth by deregulating angiogenesis. *Nature* 2006;**444**:1083–7.
20. Antonetti DA, Klein R, Gardner TW. Diabetic retinopathy. *N Engl J Med* 2012;**366**:1227–39.
21. Sava P, Ramanathan A, Dobronyi A et al. Human pericytes adopt myofibroblast properties in the microenvironment of the IPF lung. *JCI Insight* 2017;**2**:e96352.
22. Lin SL, Kisseleva T, Brenner DA et al. Pericytes and perivascular fibroblasts are the primary source of collagen-producing cells in obstructive fibrosis of the kidney. *Am J Pathol* 2008;**173**:1617–27.
23. Underly RG, Levy M, Hartmann DA et al. Pericytes as inducers of rapid, matrix Metalloproteinase-9-dependent capillary damage during ischemia. *J Neurosci* 2017;**37**: 129–40.
24. Machida T, Takata F, Matsumoto J et al. Brain pericytes are the most thrombin-sensitive matrix metalloproteinase-9-releasing cell type constituting the blood-brain barrier in vitro. *Neurosci Lett* 2015;**599**:109–14.
25. Yang D, Baumann JM, Sun YY et al. Overexpression of vascular endothelial growth factor in the germinal matrix induces neurovascular proteases and intraventricular hemorrhage. *Sci Transl Med* 2013;**5**:193ra90.
26. Dave JM, Mirabella T, Weatherbee SD et al. Pericyte ALK5/TIMP3 axis contributes to endothelial morphogenesis in the developing brain. *Dev Cell* 2018;**44**:665–78.

27. Berthiaume AA, Grant RI, McDowell KP et al. Dynamic remodeling of pericytes in vivo maintains capillary coverage in the adult mouse brain. *Cell Rep* 2018;**22**:8–16.
28. Seynhaeve ALB, Oostinga D, van Haperen R et al. Spatiotemporal endothelial cell - pericyte association in tumors as shown by high resolution 4D intravital imaging. *Sci Rep* 2018;**8**:9596.
29. Ando K, Fukuhara S, Izumi N et al. Clarification of mural cell coverage of vascular endothelial cells by live imaging of zebrafish. *Development* 2016;**143**:1328–39.
30. Eglinger J, Karsjens H, Lammert E. Quantitative assessment of angiogenesis and pericyte coverage in human cell-derived vascular sprouts. *Inflammation and Regener* 2017;**37**:2.
31. Darden J, Payne LB, Zhao H et al. Excess vascular endothelial growth factor-a disrupts pericyte recruitment during blood vessel formation. *Angiogenesis* 2018;**22**:167–83.
32. Campagnolo P, Gormley AJ, Chow LW et al. Pericyte seeded dual peptide scaffold with improved endothelialization for vascular graft tissue engineering. *Adv Healthc Mater* 2016;**5**:3046–55.
33. Brown LS, Foster CG, Courtney JM et al. Pericytes and neurovascular function in the healthy and diseased brain. *Front Cell Neurosci* 2019;**13**:282.
34. Berthiaume AA, Hartmann DA, Majesky MW et al. Pericyte structural Remodeling in cerebrovascular health and homeostasis. *Front Aging Neurosci* 2018;**10**:210.
35. Mendel TA, Clabough EB, Kao DS et al. Pericytes derived from adipose-derived stem cells protect against retinal vasculopathy. *PLoS One* 2013;**8**:e65691.
36. Brandt MM, van Dijk CGM, Maringanti R et al. Transcriptome analysis reveals microvascular endothelial cell-dependent pericyte differentiation. *Sci Rep* 2019;**9**:15586.
37. Suarez-Martinez AD, Peirce SM, Isakson BE et al. Induction of microvascular network growth in the mouse mesentery. *Microcirculation* 2018;**25**:e12502.
38. Trotter J, Karram K, Nishiyama A. NG2 cells: Properties, progeny and origin. *Brain Res Rev* 2010;**63**:72–82.
39. Suarez-Martinez AD, Bierschenk S, Huang K et al. A novel ex vivo mouse Mesometrium culture model for investigating angiogenesis in microvascular networks. *J Vasc Res* 2018;**55**:125–35.
40. Kushner EJ, Ferro LS, Yu Z et al. Excess centrosomes perturb dynamic endothelial cell repolarization during blood vessel formation. *Mol Biol Cell* 2016;**27**:1911–20.
41. Nesmith JE, Chappell JC, Cluceru JG et al. Blood vessel anastomosis is spatially regulated by Flt1 during angiogenesis. *Development* 2017;**144**:889–96.
42. Attwell D, Mishra A, Hall CN et al. What is a pericyte? *J Cereb Blood Flow Metab* 2016;**36**:451–5.
43. Robertson RT, Levine ST, Haynes SM et al. Use of labeled tomato lectin for imaging vasculature structures. *Histochem Cell Biol* 2015;**143**:225–34.
44. Yamazaki T, Nalbandian A, Uchida Y et al. Tissue myeloid progenitors differentiate into pericytes through TGF-β Signaling in developing skin vasculature. *Cell Rep* 2017;**18**:2991–3004.
45. Zhu L, Xiang P, Guo K et al. Microglia/monocytes with NG2 expression have no phagocytic function in the cortex after LPS focal injection into the rat brain. *Glia* 2012;**60**:1417–26.
46. Stefanska A, Eng D, Kaverina N et al. Interstitial pericytes decrease in aged mouse kidneys. *Aging (Albany NY)* 2015;**7**:370–82.
47. Sagare AP, Bell RD, Zhao Z et al. Pericyte loss influences Alzheimer-like neurodegeneration in mice. *Nat Commun* 2013;**4**:2932.
48. Lindblom P, Gerhardt H, Liebner S et al. Endothelial PDGF-B retention is required for proper investment of pericytes in the microvessel wall. *Genes Dev* 2003;**17**:1835–40.
49. Hellstrom M, Kalen M, Lindahl P et al. Role of PDGF-B and PDGFR-beta in recruitment of vascular smooth muscle cells and pericytes during embryonic blood vessel formation in the mouse. *Development* 1999;**126**:3047–55.
50. Stratman AN, Schwindt AE, Malotte KM et al. Endothelial-derived PDGF-BB and HB-EGF coordinately regulate pericyte recruitment during vasculogenic tube assembly and stabilization. *Blood* 2010;**116**:4720–30.
51. Gibson WT, Veldhuis JH, Rubinstein B et al. Control of the mitotic cleavage plane by local epithelial topology. *Cell* 2011;**144**:427–38.
52. Mochizuki T, Suzuki S, Masai I. Spatial pattern of cell geometry and cell-division orientation in zebrafish lens epithelium. *Biol Open* 2014;**3**:982–94.
53. Fink J, Carpi N, Betz T et al. External forces control mitotic spindle positioning. *Nat Cell Biol* 2011;**13**:771–8.
54. Thery M, Racine V, Pepin A et al. The extracellular matrix guides the orientation of the cell division axis. *Nat Cell Biol* 2005;**7**:947–53.
55. Chappell JC, Mouillesseaux KP, Bautch VL. Flt-1 (vascular endothelial growth factor receptor-1) is essential for the vascular endothelial growth factor-notch feedback loop during angiogenesis. *Arterioscler Thromb Vasc Biol* 2013;**33**:1952–9.
56. Kappas NC, Zeng G, Chappell JC et al. The VEGF receptor Flt-1 spatially modulates Flk-1 signaling and blood vessel branching. *J Cell Biol* 2008;**181**:847–58.
57. Kelly-Goss MR, Sweat RS, Stapor PC et al. Targeting pericytes for angiogenic therapies. *Microcirculation* 2014;**21**:345–57.
58. Stapor PC, Sweat RS, Dashti DC et al. Pericyte dynamics during angiogenesis: New insights from new identities. *J Vasc Res* 2014;**51**:163–74.
59. Stapor PC, Murfee WL. Identification of class III beta-tubulin as a marker of angiogenic perivascular cells. *Microvasc Res* 2012;**83**:257–62.
60. Murfee WL, Rehorn MR, Peirce SM et al. Perivascular cells along venules upregulate NG2 expression during microvascular remodeling. *Microcirculation* 2006;**13**:261–73.
61. Blancas AA, Wong LE, Glaser DE et al. Specialized tip/stalk-like and phalanx-like endothelial cells from embryonic stem cells. *Stem Cells Dev* 2013;**22**:1398–407.
62. Mazzone M, Dettori D, Leite de Oliveira R et al. Heterozygous deficiency of PHD2 restores tumor oxygenation and inhibits metastasis via endothelial normalization. *Cell* 2009;**136**:839–51.
63. Ubezio B, Blanco RA, Geudens I et al. Synchronization of endothelial Dll4-notch dynamics switch blood vessels from branching to expansion. *Elife* 2016;**5**:e12167.
64. Bergers G, Song S. The role of pericytes in blood-vessel formation and maintenance. *Neuro Oncol* 2005;**7**:452–64.
65. Hosaka K, Yang Y, Seki T et al. Pericyte-fibroblast transition promotes tumor growth and metastasis. *Proc Natl Acad Sci U S A* 2016;**113**:E5618–27.
66. Birbrair A, Zhang T, Files DC et al. Type-1 pericytes accumulate after tissue injury and produce collagen in an organ-dependent manner. *Stem Cell Res Ther* 2014;**5**:122.
67. Simons M, Alitalo K, Annex BH et al. State-of-the-art methods for evaluation of angiogenesis and tissue vascularization: A scientific statement from the American Heart Association. *Circ Res* 2015;**116**:e99–132.